Front. Optoelectron. China 2010, 3(3): 321–327
DOI 10.1007/s12200-010-0102-0

RESEARCH ARTICLE

Investigation of Al Schottky junction on n-type CdS film deposited on polymer substrate

Sandhya GUPTA (✉), Dinesh PATIDAR, Mahesh BABOO, Kananbala SHARMA, N. S. SAXENA

Semiconductor and Polymer Science Laboratory, University of Rajasthan, Jaipur 302055, India

Abstract A systematic study has been made on the behavior of Al/n-CdS thin film junction on flexible polymer substrate (polyethylene terephthalate, PET) grown using thermal evaporation method. Temperature dependence of $I-V$ measurements for this junction has been done which closely follow the equations of Schottky barrier junction dominated by thermionic emission mechanism. Intrinsic and contact properties such as barrier height, ideality factor and series resistance have been calculated from $I-V$ characteristics. The barrier height of Al/n-CdS junction is found to increase with increase in temperature whereas ideality factor and series resistance decrease with increase in temperature.

Keywords polymer substrate, Al/n-CdS thin film, thermal evaporation method, Schottky barrier junction

1 Introduction

The electrical and optical properties of the II-VI compound semiconductors have been the subject of a variety of investigations over the past 30 years and have resulted in a number of device applications. In particular, evaporated CdS film has been used as ultrasonic transducers, photo resistors, luminescent layers and heterojunction diodes [1–3]. As a result, numerous structural, electrical and optical studies of thin films have been made in view of improving the performance of the devices or finding a new area of application.

CdS thin films can be prepared by different techniques [4–11] such as thermal evaporation, close spaced sublimation, metal organic chemical vapor deposition (MOCVD), molecular-beam epitaxy (MBE), chemical bath deposition (CBD), chemical spray pyrolysis (CSP), electrodeposition and sputtering. Among these methods, thermal evaporation is one of the suitable methods for depositing large area thin film for solar cell application [12]. The development of CdS films on flexible substrates is gaining interest due to the light weight and damage free nature of the devices. Light weight CdS solar cells on flexible polymer substrates are very attractive for space applications [13].

CdS/metal Schottky junctions on light weight flexible polymer substrates may prove to be a very attractive approach for electrical application due to the above said properties. Thus, efforts have been made to study the properties of the interfaces through the measurements of $I-V$ characteristics in Au-CdS junction by Chavez et al. [12] and by Patel et al. [14]. Also, electrical studies have been made by Gupta et al. [15] for Cu-CdS and Zn-CdS Schottky junctions by determining various junction parameters. Electrical and photovoltaic characteristics of Al/n-CdS Schottky junction have been made by Farag et al. [16]. However, very little effort has been made to study the temperature dependent junction parameters of Al/CdS Schottky junction.

In this present work, an attempt has been made to study the $I-V$ characteristics of Al/n-CdS thin film junction grown by thermal evaporation method on flexible polymer substrate (polyethylene terephthalate, PET). $I-V$ characteristics of this junction have been carried out in a temperature range of 300 to 350 K using Keithley electrometer. An effort has also been made to see the effect of temperature on junction parameter such as barrier height, ideality factor, saturation current and series resistance.

2 Experimental details

2.1 Thin film junction preparation

CdS thin film of area 2.25 cm^2 has been grown on PET substrate using evaporation of CdS powder (99.999% pure,

Received February 20, 2010; accepted March 22, 2010

E-mail: 1982sanman@gmail.com

from Alfa Aesar) in a residual pressure of 10^{-5} Torr. Cleaned PET film of thickness 20 μm (from Good Fellow Cambridge Limited, England) has been used as substrate while molybdenum is used as boat source. The thickness of CdS film has been measured by Quartz crystal thickness monitor (Model CTM 200) and is found to be of the order of 330 nm.

After the deposition of CdS film over PET substrate, an aluminum film of area 0.5625 cm^2 is deposited over the CdS film just by breaking the vacuum in the chamber and then again restoring it to 10^{-5} Torr for the deposition of aluminum film. The thickness of Al-film deposited over the CdS film is found to be 120 nm. Indium electrodes have been fabricated over CdS and aluminum films to have good electrical contacts as shown in Fig. 1.

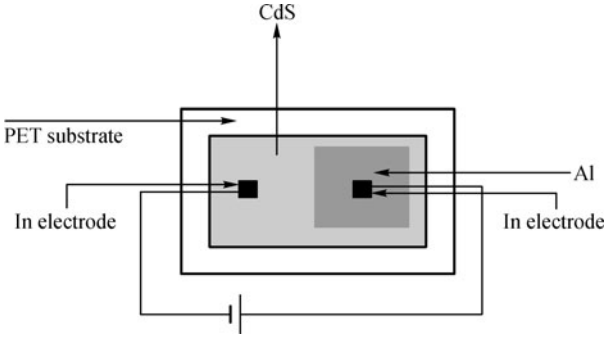

Fig. 1 Schematic diagram of Al/n-CdS junction

2.2 Characterization study

A structural study of CdS-PET film was done using X-ray diffraction pattern performed with Philips X'pert X-ray diffractometer at a scanning rate of 3° per minute between 10° to 60°. The source used throughout this study was Cu Kα (λ = 1.5406×10^{-10} m) operated at 40 mA and 45 kV. Scanning electron microscopy (SEM) of PET and CdS-PET films was performed using FEI Quanta 200 F equipment for determination of surface morphology of the coated layer. The PET sample was gold-sputtered prior to measurements.

2.3 Electrical study

$I-V$ characteristics of Al/n-CdS Schottky junction were carried out by Keithley Electrometer/High Resistance meter 6517 A at the temperatures of 300, 310, 320, 330, 340 and 350 K. The electrical contacts were made on indium electrodes. The Keithley electrometer has an in built capacity of output independent voltage source of ±1000 V. The voltage was applied across the sample to measure the current through the sample.

3 Results and discussion

3.1 Structural analysis

An X-ray diffraction (XRD) pattern provides valuable information about the structure of a sample. Figure 2 shows the X-ray diffraction patterns of PET and CdS-PET films.

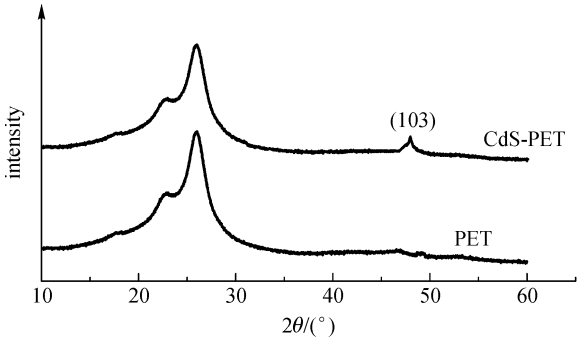

Fig. 2 XRD patterns of PET and CdS-PET film

Figure 2 shows the semicrystalline nature of PET film [17]. The XRD pattern of CdS-PET film also shows a peak of CdS material. It reveals that CdS has a hexagonal structure with primitive lattice having a cell parameter of $a = 4.136\times10^{-10}$ m, $c = 6.713\times10^{-10}$ m and preferred (103) orientation of micro crystallites. The grain size of the crystallites (G) has been estimated using the following relation [18]:

$$G = \frac{k\lambda}{\beta\cos\theta}, \tag{1}$$

where k is shape factor (it is the ratio of major to minor dimension of a particle which varies between 0.9 and 1.0 depending on the shape of the particle), λ is the wavelength of X-ray used, θ is the Bragg's angle and β is the full width at half maximum (FWHM) of the peak. The average grain size of CdS particle is found to be 17 nm.

Figures 3(a) and 3(b) show the SEM images of PET and CdS-PET films. The CdS-PET film shows a continuous globular structure on the surface while the PET film presents a planner sheet structure. SEM images show the diffusion of the coating material into the base film, which can affect the electrical properties of the film.

3.2 Electrical analysis

$I-V$ characteristics of Al/n-CdS junction show the rectification behavior which indicates the formation of Schottky contact between Al and CdS film. $I-V$ characteristic of this Schottky junction at room temperature (300 K) is shown in Fig. 4.

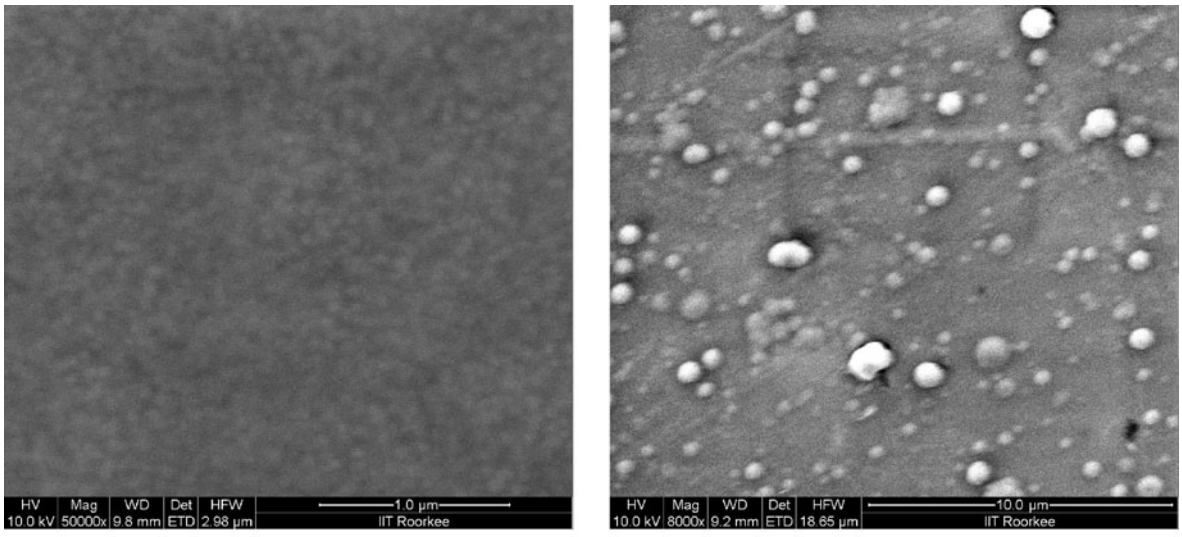

Fig. 3 SEM images of (a) PET and (b) CdS-PET films

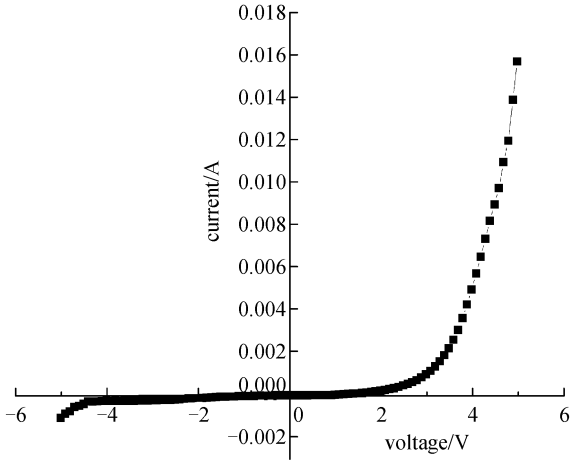

Fig. 4 I–V characteristic of Al/n-CdS Schottky junction at room temperature

ln$I$– V characteristic of Al/n-CdS Schottky junction at various temperatures for forward and reverse bias in the range 300–350 K are shown in Figs. 5(a) and 5(b), respectively. Theoretically, the current transport through Schottky barrier junction under a forward bias 'V' in thermionic emission is given by the relation [19] below:

$$I = I_s\left[\exp\left(\frac{eV}{nk_BT}\right) - 1\right], \tag{2}$$

$$I_s = A^*T^2\exp\left(-\frac{e\Phi_b}{k_BT}\right), \tag{3}$$

where e is the charge on electron, V is the applied voltage, n is the diode ideality factor, k_B is the Boltzmann constant, T is the temperature, Φ_b is the effective barrier height, $A^* = 12\ \mathrm{A\cdot cm^{-2}\cdot K^{-2}}$ is the effective Richardson constant and I_s is the reverse saturation current.

The ideality factor, n can be obtained from Eq. (4) as given here

$$n = \frac{e}{k_BT}\frac{dV}{d(\ln I)}. \tag{4}$$

To determine the ideality factor, n of the junction a curve between ln$I$ versus voltage has been plotted for different temperatures (Fig. 6) in the range of 0.0–0.3 V. The slope of the curves is calculated in the region 0.08 V to 0.22 V, which further helps in the determination of n at different temperatures. The reverse saturation current (I_s) was obtained by extrapolating the straight line portion (in reverse bias) of I–V curve to $V = 0$.

Using the value of I_s, the apparent barrier height can be computed using the relationship:

$$\Phi_b = \frac{k_BT}{e}\ln\frac{A^*T^2}{I_s}, \tag{5}$$

$$\ln\frac{I_s}{T^2} = \ln A^* - \frac{e\Phi_b}{k_BT}. \tag{6}$$

To identify the dominant current transport through the junction, lnI_s has been plotted as a function of inverse temperature (Richardson plot) and is shown in Fig. 7. The variation has been found to be linear in the entire range. This indicates that thermionic emission is the dominant mechanism of charge transport. The barrier height (Φ_b) and Richardson constant (A^*) have been calculated from the slope and the intercept of the Richardson plot. The

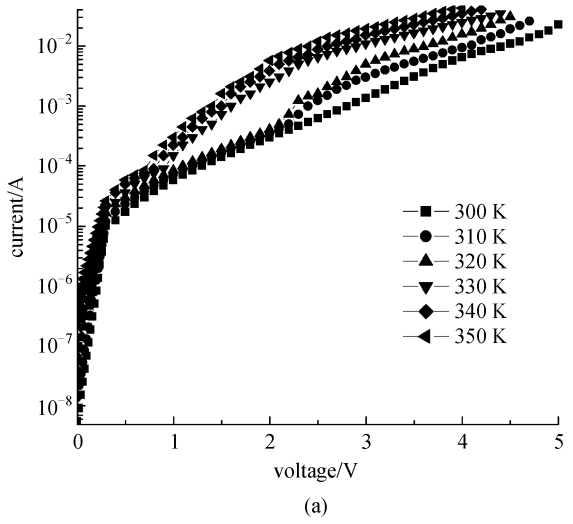

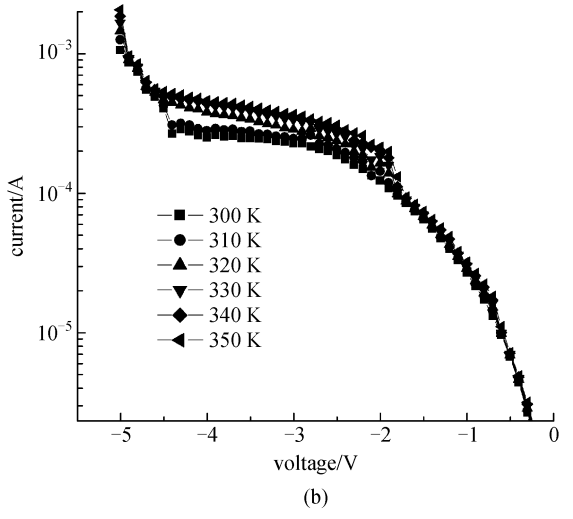

Fig. 5 I–V characteristic of Al/n-CdS Schottky junction at various temperatures for (a) forward and (b) reverse bias

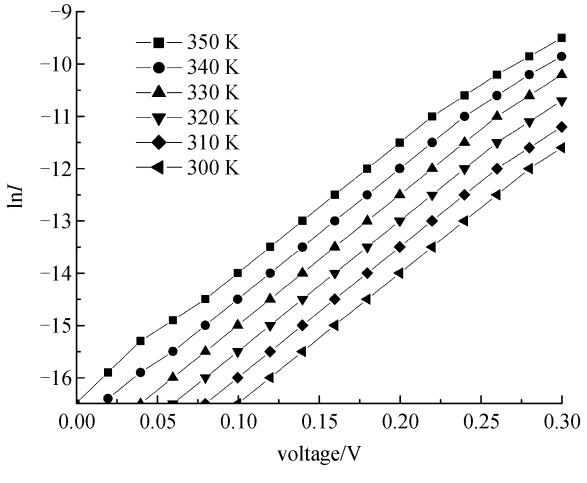

Fig. 6 ln$I$ versus voltage curve for Al/n-CdS junction for different temperatures

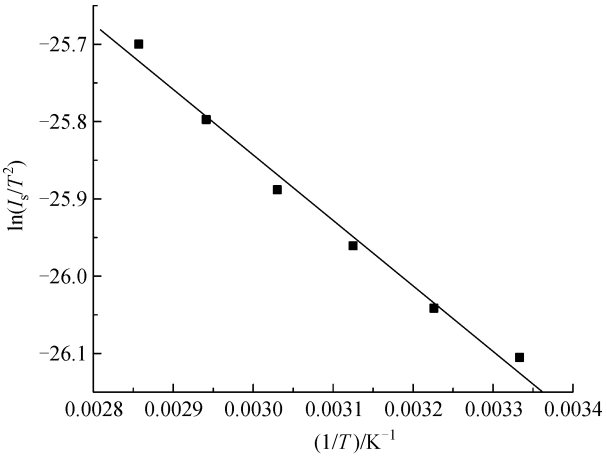

Fig. 7 Richardson plot of Al/n-CdS Schottky junction

obtained value of A^* is 0.076×10^{-8} A·cm^{-2}·K^{-2}, which is much lower than the theoretical value of $A^* = 12$ A·cm^{-2}·K^{-2} for n-CdS. The A^* value obtained from the temperature dependence of the I–V characteristics may be affected by lateral inhomogeneity of the barrier [20]. The value of Φ_b obtained from Fig. 7 is 0.112 eV. The value of Φ_b has also been obtained from Eq. (5) using theoretical value of A^* at different temperatures and is given in Table 1.

The dependence of barrier height (calculated from theoretical value of A^*) and ideality factor on temperature is shown in Fig. 8. It has been observed that the value of ideality factor decreases from 1.54 to 1.32 with increase in temperature from 300 to 350 K. On the other hand, barrier height increases with increase in temperature, i.e., its value increases from 0.74 to 0.85 on increasing temperature from 300 to 350 K. The experimental values of barrier height are in good agreement with the values reported by Farag et al. [16] for Al/n-CdS Schottky junction.

The ideality factor of the junctions studied in the present work is found to be greater than unity. An ideality factor greater than unity is generally attributed to the presence of a bias-dependent Schottky barrier height. The barrier height varies with applied voltage because conduction electrons experience a force from their image charges in the metal. This force attracts the electrons toward the metal surface, effectively lowering the barrier and allowing voltage dependent deviations. Tunneling, generation-recombination and interface impurities are possible factors, which could lead to a higher ideality factor [21].

The dependence of Schottky barrier height (SBH) on temperature can be understood by the lateral SBH inhomogeneities model as proposed by Tung [22–24], Werner and Güttler [25]. This model (parallel conduction model) explains well the dependence of SBH and ideality factor on temperature by considering the SBH inhomogeneities at the metal-semiconductor (MS) interface in nanometer length scales. Since current transport across the

Table 1 Values of various Al/n-CdS junction parameter

temperature/K	n	I_s/A	Φ_b/eV	R_s/Ω
300	1.54	4.14×10^{-7}	0.74	130
310	1.49	4.71×10^{-7}	0.76	100
320	1.45	5.44×10^{-7}	0.78	70
330	1.40	6.22×10^{-7}	0.80	50
340	1.36	7.23×10^{-7}	0.83	40
350	1.32	8.45×10^{-7}	0.85	33

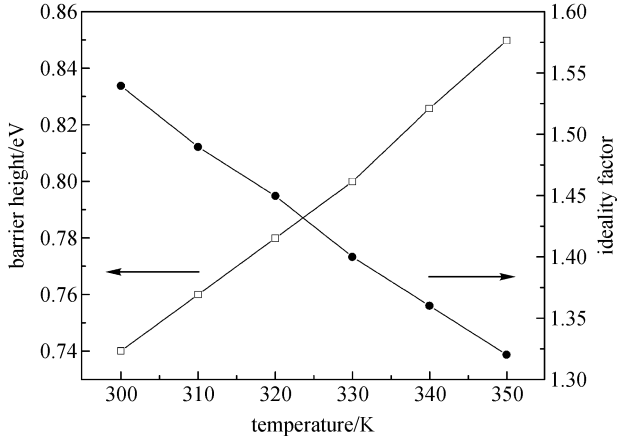

Fig. 8 Barrier height and ideality factor of Al/n-CdS junction for different temperatures

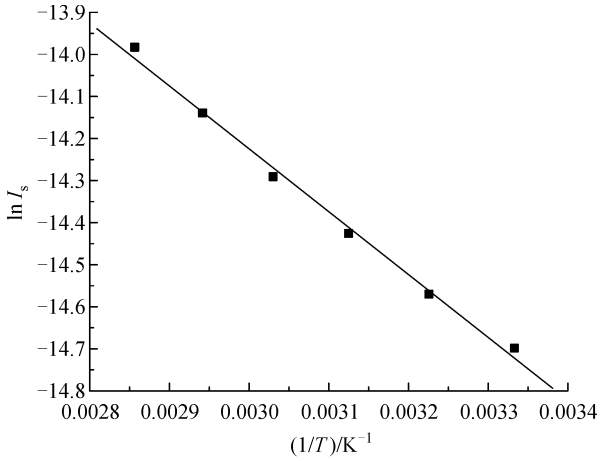

Fig. 9 $\ln I_s$ versus $1/T$ curve for Al/n-CdS junction (slope is $-E_a/k$)

metal/semiconductor interface is a temperature activated process, at low temperatures electrons are able to surmount the lower barriers and therefore the current transport will be dominated by current flowing through the patches of lower SBH and a larger ideality factor is obtained [26,27]. As the temperature increases, more and more electrons have sufficient energy to surmount the higher barrier and hence conduction increases with decreasing ideality factor. A Gaussian distribution of the barrier heights based on thermionic emission mechanism has been widely accepted and utilized to explain the nature of this temperature dependence by some studies [28,29].

For a thermally activated phenomenon, I_s is expressed as

$$I_s = I_{so}\exp\left(-\frac{E_a}{kT}\right), \tag{7}$$

where E_a is the thermal activation energy of the process. If the current transport is due to diffusion, n is equal to 1 and the activation energy is equal to the band gap of the semiconductor [30]. But in the present study, the activation energy calculated by Fig. 9 is 0.13 eV which is much lower than the CdS band gap (2.42 eV) suggesting that the thermionic emission mechanism may be the dominant mechanism for current transport in this range as indicated by the observed linearity in $\ln I - V$ plots (Fig. 5) [21].

The series resistance (R_s) can be determined independently from the I versus V plot in the high forward bias region. Figure 10 shows the series resistance values calculated from forward $I-V$ characteristics as a function of temperature. The R_s values vary exponentially with temperature and the value decreases from 130 to 40 Ω in the temperature range 300 to 350 K. The decrease of R_s with increasing temperature is attributed to the factors

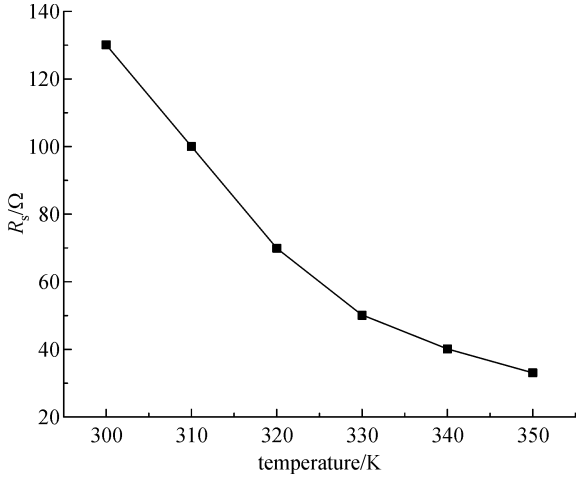

Fig. 10 Variation of series resistance of Al/n-CdS junction with temperature

responsible for the increase of n. The change in junction parameters of Al/n-CdS Schottky junction with temperature is shown in Table 1.

4 Conclusions

A systematic study on the effect of temperature on the $I-V$ characteristics of the Al/n-CdS Schottky junction leads to the following conclusions: a) the dominant conduction mechanism in the forward bias region seems to be thermionic emission; b) the barrier height and saturation current of Al/n-CdS junction increase with increase in temperature whereas ideality factor and series resistance decrease with increase in temperature.

Acknowledgements One of the authors Sandhya Gupta is thankful to the University Grant Commission for providing financial assistance during this work. The authors would also like to thank Ms. Deepika, Ms. Manasvi Dixit, Mrs. Faheem Naqvi, Mr. K. S. Rathore, and Mr. Vishal Mathur for their help in various ways during the course of this work.

References

1. DeKlerk J, Kelly R F. Vapor-deposited thin film piezoelectric transducers. Review of Scientific Instruments, 1965, 36(4): 506–510
2. Andrews A M, Haden C R. Electroluminescence in vacuum evaporated cadmium sulfide. Proceedings of the IEEE, 1969, 57 (1): 99–100
3. Dresner J, Shallcross F V. Ractification and space-charge-limited currents in CdS films. Solid-State Electronics, 1962, 5(4): 205–210
4. Mohanchandra K P, Uchil J. Electrical properties of CdS and CdSe films deposited on vibrating substrates. Journal of Applied Physics, 1998, 84(1): 306–310
5. Ferekides C S, Marinskiy D, Marinskaya S, Tetali B, Oman D, Morel D L. CdS films prepared by the close-spaced sublimation and their influence on CdTe/CdS solar cell performance. In: Proceedings of the Twenty Fifth IEEE Photovoltaic Specialists Conference. 1996, 751–756
6. Uda H, Yonezawa H, Ohtsubo Y, Kosaka M, Sonomura H. Thin CdS films prepared by metalorganic chemical vapor deposition. Solar Energy Materials and Solar Cells, 2003, 75(1–2): 219–226
7. Fujita S, Kawakami Y. MO(GS)MBE and photo-MO(GS)MBE of II-VI semiconductors. Journal of Crystal Growth, 1996, 164(1–4): 196–201
8. Gluszak E A, Hinckley S. Growth of ultrathin chemically-deposited CdS films from an ammonia-thiourea reaction system. In: Proceedings of Conference on Optoelectronic and Microelectronic Materials and Devices. 2000, 218–221
9. Pence S, Bates C W Jr, Varner L. Morphological features in films of CdS prepared by chemical spray pyrolysis. Materials Letters, 1995, 23(4–6): 195–201
10. Anuar K, Zulkarnain Z, Saravanan N, Nazri M, Sharin R. Effects of electrodeposition periods and solution temperatures towards the properties of CdS thin films prepared in the presence of sodium Tartrate. Materials Science, 2005, 11(2): 101–104
11. Lee J H, Lee D J. Effects of $CdCl_2$ treatment on the properties of CdS films prepared by r.f. magnetron sputtering. Thin Solid Films, 2007, 515(15): 6055–6059
12. Chavez H, Jorden M, McClure J C, Lush G, Singh V P. Physical and electrical characterization of CdS films deposited by vacuum evaporation, solution growth and spray pyrolysis. Journal of Materials Science Materials in Electronics, 1997, 8(3): 151–154
13. Mathew X, Enriquez J P, Romeo A, Tiwari A N. CdTe/CdS solar cells on flexible substrates. Solar Energy, 2004, 77(6): 831–838
14. Patel B K, Nanda K K, Sahu S N. Interface characterization of nanocrystalline CdS/Au junction by current-voltage and capacitance-voltage studies. Journal of Applied Physics, 1999, 85(7): 3666–3670
15. Gupta S, Patidar D, Saxena N S, Sharma K, Sharma T P. Electrical study of Cu-CdS and Zn-CdS Schottky junction. Optoelectronics and Advanced Materials—Rapid Communications, 2008, 2(4): 205–208
16. Farag A A M, Yahia I S, Fadel M. Electrical and photovoltaic characteristics of Al/n-CdS Schottky diode. International Journal of Hydrogen Energy, 2009, 34(11): 4906–4913
17. Callister W D. Materials Science and Engineering: An Introduction, in Characteristics, Applications and Processing of Polymers. New York: John Wiley & Sons, 2000
18. Lalitha S, Sathyamoorthy R, Senthilarasu S, Subbarayan A, Natarajan K. Characterization of CdTe thin film—dependence of structural and optical properties on temperature and thickness. Solar Energy Materials and Solar Cells, 2004, 82(1–2): 187–199
19. Sze S M. Physics of Semiconductor Devices. 2nd ed. New York: Wiley Interscience, 1981, 255
20. Gümüs A, Türüt A, Yalcin N. Temperature dependent barrier characteristics of CrNiCo alloy Schottky contacts on n-type molecular epitaxy GaAs. Journal of Applied Physics, 2002, 91(1): 245–250
21. Chand S, Kumar J. Current-voltage characteristics and barrier parameters of Pd2Si/p-Si(111) Schottky diodes in a wide temperature range. Semiconductor Science and Technology, 1995, 10(12): 1680–1688
22. Tung R T. Electron transport of inhomogeneous Schottky barriers. Applied Physics Letters, 1991, 58(24): 2821–2823
23. Tung R T. Electron transport at metal-semiconductor interfaces: general theory. Physical Review B, 1992, 45(23): 13509–13523
24. Tung R T, Levi A F, Sullivan J P, Schrey F. Schottky-barrier inhomogeneity at epitaxial $NiSi_2$ interfaces on Si(100). Physical Review Letters, 1991, 66(1): 72–75
25. Werner J H, Güttler H H. Barrier inhomogeneities at Schottky contacts. Journal of Applied Physics, 1991, 69(3): 1522–1533
26. Sullivan J P, Tung R T, Pinto M R, Graham W R. Electron transport of inhomogeneous Schottky barriers: a numerical study. Journal of Applied Physics, 1991, 70(12): 7403–7424
27. Pattabi M, Krishnan S, Ganesh, Mathew X. Effect of temperature and electron irradiation on the $I-V$ characteristics of Au/CdTe Schottky diodes. Solar Energy, 2007, 81(1): 111–116
28. Zhu S, Van Meirhaeghe R L, Detavernier C, Cardon F, Ru G P, Qu X P, Li B Z. Barrier height inhomogeneities of epitaxial $CoSi_2$ Schottky contacts on n-Si (100) and (111). Solid-State Electronics,

2000, 44(4): 663–671

29. Karadeniz S, Sahin M, Tugluoglu N, Safak H. Temperature dependent barrier characteristics of Ag/p-SnS Schottky barrier diodes. Semiconductor Science and Technology, 2004, 19(9): 1098–1103

30. Marsal L F, Pallarès J, Correig X, Orpella A, Bardés D, Alcubilla R. Current transport mechanisms in n-type amorphous silicon carbon on p-type crystalline silicon (a-$Si_{0.8}C_{0.2}$:H/c-Si) heterojunction diodes. Semiconductor Science and Technology, 1998, 13(10): 1148–1153